MOLECULAR AND CELLULAR BIOLOGY, Dec. 2006, p. 9352–9363 Vol. 26, No. 24
0270-7306/06/$08.00+0 doi:10.1128/MCB.01148-06

Neuromedin U Receptor 2-Deficient Mice Display Differential Responses in Sensory Perception, Stress, and Feeding▽

Hongkui Zeng,[1]* Alexander Gragerov,[1]† John G. Hohmann,[1]‡ Maria N. Pavlova,[1]† Brian A. Schimpf,[1] Hui Xu,[2] Long-Jun Wu,[2] Hiroki Toyoda,[2] Ming-Gao Zhao,[2] Alex D. Rohde,[1]† Galina Gragerova,[1]† Rene Onrust,[1]† John E. Bergmann,[1]† Min Zhuo,[2] and George A. Gaitanaris[1]†

Nura, Inc., 1124 Columbia Street, Seattle, Washington 98104,[1] and Department of Physiology, Faculty of Medicine, University of Toronto, University of Toronto Centre for the Study of Pain, 1 King's College Circle, Toronto, Ontario M5S 1A8, Canada[2]

Received 26 June 2006/Returned for modification 17 August 2006/Accepted 22 September 2006

Neuromedin U (NMU) is a highly conserved neuropeptide with a variety of physiological functions mediated by two receptors, peripheral NMUR1 and central nervous system NMUR2. Here we report the generation and phenotypic characterization of mice deficient in the central nervous system receptor NMUR2. We show that behavioral effects, such as suppression of food intake, enhanced pain response, and excessive grooming induced by intracerebroventricular NMU administration were abolished in the NMUR2 knockout (KO) mice, establishing a causal role for NMUR2 in mediating NMU's central effects on these behaviors. In contrast to the NMU peptide-deficient mice, NMUR2 KO mice appeared normal with regard to stress, anxiety, body weight regulation, and food consumption. However, the NMUR2 KO mice showed reduced pain sensitivity in both the hot plate and formalin tests. Furthermore, facilitated excitatory synaptic transmission in spinal dorsal horn neurons, a mechanism by which NMU stimulates pain, did not occur in NMUR2 KO mice. These results provide significant insights into a functional dissection of the differential contribution of peripherally or centrally acting NMU system. They suggest that NMUR2 plays a more significant role in central pain processing than other brain functions including stress/anxiety and regulation of feeding.

Neuromedin U (NMU) is a highly conserved neuropeptide, present in various species from amphibians to mammals (reviewed in reference 3). In humans, NMU is a 25-amino-acid (aa) peptide (NMU-25), and in rodents, it is a 23-aa peptide (NMU-23), whereas in some other mammalian species an 8-aa peptide (NMU-8) has also been found. NMU-8 is identical to the C terminus of NMU-25, which is the most highly conserved region of the entire peptide, and has receptor affinity in vitro similar to that of NMU-25. NMU is widely distributed in the body, with the most abundant expression in the gastrointestinal tract, anterior pituitary, spinal cord, brain, and genitourinary tract (6, 42). Correspondingly, NMU has been implicated in regulating a variety of physiological functions, including smooth-muscle contraction, blood pressure regulation, stress response, feeding and energy homeostasis, nociception, and circadian rhythm (reviewed in reference 3).

Two G-protein-coupled receptors, NMUR1 and NMUR2, have been identified as the receptors for NMU (8, 18, 20, 21, 37, 41, 42). The two receptors belong to the rhodopsin-like class A G-protein-coupled receptors family and share ~50% identity with each other in the seven-transmembrane region. The tissue distribution of the two receptors is quite distinct and complementary to each other: NMUR1 is expressed predominantly in the periphery, with highest levels in the gastrointestinal tract (8, 10, 18, 42), whereas NMUR2 is predominantly expressed in the central nervous system, with greatest expression in regions of hypothalamus, medulla, and spinal cord (9, 10, 14, 20, 21, 41).

In the brain, NMU is expressed in hypothalamic regions associated with regulation of food intake and energy homeostasis, such as the arcuate nucleus (13, 21). Also, *Nmur2* is present in the hypothalamic paraventricular nucleus (PVN) in rats and in the arcuate nucleus in mice (13, 21). *Nmu* mRNA in ventromedial hypothalamus is significantly decreased in fasting rats (21). Central administration of NMU inhibits food intake and stimulates energy expenditure in rats (21, 23, 27, 34) and mice (17). Central injection of anti-NMU antibody increases food intake (27). Transgenic mice with ubiquitous overexpression of NMU are hypophagic, lean, and have improved glucose tolerance (28). On the other hand, NMU knockout (KO) mice are hyperphagic, hypoactive, hypometabolic, and obese (16). These data suggest that NMU is an important regulator of energy balance.

The expression of *Nmur2* in hypothalamic PVN, a major site for the release of corticotrophin-releasing hormone (CRH), suggests that NMU may also have a role in mediating stress response. Indeed, administration of NMU directly into PVN increases plasma levels of adrenocorticotrophin and corticosterone, and NMU stimulates the release of CRH from hypothalamic explants in vitro (45, 50). Central administration of NMU also induces c-Fos expression in hypothalamic areas associated with stress (23, 35, 36) as well as stress-related behaviors that can be blocked by CRH antagonist or anti-CRH antibody and is absent from CRH KO mice (15). Certain stress responses are abolished in the NMU KO mice (33).

NMU and its receptors are also abundantly expressed in

* Corresponding author. Present address: Omeros Corporation, 1124 Columbia Street, Seattle, WA 98104. Phone: (206) 344-2072. Fax: (206) 344-2101. E-mail: hzeng@omeros.com.

† Present address: Omeros Corporation, 1124 Columbia Street, Seattle, WA 98104.

‡ Present address: Allen Institute for Brain Science, 551 N. 34th Street, Seattle, WA 98103.

▽ Published ahead of print on 9 October 2006.

nociceptive sensory pathways, including the dorsal root ganglia (DRG), spinal cord, and brainstem (19, 30, 51). In particular, both *Nmur2* expression and NMU-23 binding sites are highly localized to the outer layers of the spinal dorsal horn, whereas *Nmur1* is expressed in about 25% small/medium-diameter neurons in the DRG (51). Central administration of NMU via intrathecal (i.t.) or intracerebroventricular (i.c.v.) injections increases pain sensitivity in rats and mice. NMU induces thermal hyperalgesia, mechanical allodynia, and increased persistent pain after formalin injection (4, 33, 51). Both i.c.v. and i.t. injections of NMU in rats and mice induce behavior responses associated with activation of the nociceptive pathways (4, 51). NMU KO mice exhibit reduced pain sensitivity in both hot plate test and the chronic phase of the formalin test (33). These results suggest that NMU significantly modulates nociceptive sensory transmission.

Given the distinct expression patterns of the two receptors for NMU, we postulated that the central nervous system functions of NMU, such as feeding, stress, and nociception, may be mediated mainly by NMUR2. However, there has been no evidence to date to show how the two receptors may be involved in the different aspects of the function of NMU. In an effort to delineate the selective roles of NMUR2, we describe here the generation and comprehensive analysis of the NMUR2 null mutant (KO) mice. We show that NMUR2 KO mice have a specific alteration in pain sensation while being largely normal in all other behavioral aspects examined, including body weight and food intake. We also show that NMUR2 is necessary for all the behavioral effects of central nervous system administration of NMU, including hyperalgesia and suppression of feeding. Thus, NMUR2 plays a major role in mediating NMU's neural function, most prominently in the nociceptive sensory perception.

MATERIALS AND METHODS

Experimental animals. Mice were kept on a constant light/dark cycle (12:12 with lights on at 7 a.m. and off at 7 p.m.) with ad libitum food and water access. Mice were weaned onto PicoLab Mouse Diet 20 (20% protein, 9% fat). Only male mice were used in all studies. All experimental procedures were approved by the Institutional Animal Care and Use Committees of Nura, Inc., and University of Toronto in accordance with the National Institutes of Health Guide to Care and Use of Laboratory Animals.

Generation of NMUR2 KO mice. NMUR2 KO mice were produced by retroviral mutagenesis as described previously (29). Briefly, an embryonic stem (ES) cell library was constructed by infecting 129Sv ES cells with a retroviral vector (11). Mutations in the *Nmur2* gene were found in the library by PCR analysis of genomic DNA using vector-specific and gene-specific primers. Mutant clones isolated from the library were used for animal production using standard methods. Chimeric mice were bred with 129S1/SvImJ mice to generate heterozygotes in an inbred background. The resulting progeny were genotyped by PCR of tail DNA to identify pups containing a disruption in the *Nmur2* gene. Using Southern blotting, two viral insertions were found present in the mutant mice, one in the *Nmur2* gene and another somewhere else in the genome. After several generations of selective breeding for mutation in *Nmur2*, the second random insertion was bred out.

For phenotypic studies, heterozygous males in 129S1/SvImJ inbred background were bred with C57BL/6J females to obtain 129/B6 F_1 hybrid heterozygous mice, which were then bred with each other to obtain homozygous *Nmur2* KO mice and wild-type (WT) control littermates in a 129/B6 F_2 hybrid background.

Reverse transcriptase PCR (RT-PCR) was employed to confirm inactivation of the *Nmur2* gene. Brains were dissected and stored in RNALater (Ambion, Austin, TX) at 4°C until RNA isolation. Total RNA was isolated using Totally RNA kit (Ambion) and treated with DNase I (Ambion) for 1 h at 37°C. An equal amount (~100 ng) of total RNA was used in each sample for reverse transcription reactions using a Super-Script first-strand synthesis kit (Invitrogen, Carlsbad, CA). Each reaction was run in duplicate with (RT+) or without (RT−) RT to control for possible genomic DNA contamination. cDNA was amplified for 40 cycles (94°C for 30 s, 56°C for 40 s, 72°C for 90 s, final extension of 72°C for 7 min) with *Nmur2*-specific primers (primer a in exon 1, 5′-TGCTGGTCCTGCT CTTAGGTATGCC-3′ and primer b in exon 4 5′-GAACTGGGGGCCCGCAT CCT-3′) to produce a predicted 870-bp PCR fragment.

Receptor binding of radiolabeled NMU peptide to spinal cord sections was used to confirm the functional loss of NMUR2 protein. The lumbar spinal cord was dissected along with surrounding bones and quickly frozen on dry ice. The frozen spinal cord was sectioned transversely at 14 μm in a cryostat. The slides were preincubated at room temperature for 20 min in binding buffer (50 mM Tris-HCl, pH 7.5, 5 mM $MgCl_2$, 2 mM EGTA, 0.01% Tween 20) and then for 10 min in binding buffer plus 5 mg/ml bovine serum albumin (BSA) and 10 mM phenylmethylsulfonyl fluoride. The slides were then covered with 100 μl of the buffer with BSA and phenylmethylsulfonyl fluoride supplemented with ~1 pmol of ^{125}I-NMU-23 (specific activity, ~1,300 Ci/mmol; Phoenix Pharmaceuticals, Belmont, CA). For nonspecific binding control, 1 nmol (1,000× excess) of unlabeled NMU-8 peptide (Phoenix Pharmaceuticals) was added to the above solution containing ^{125}I-NMU-23. Binding was allowed to occur for 1 h at room temperature. The slides were then washed 3 times, 4 min each, with ice-cold binding buffer plus 1 mg/ml BSA, briefly dipped in ice-cold water, and air-dried for a few hours. Dry slides were exposed for 8 days with a Kodak BioMax MR film, and the resulting autoradiograms were photographed under a microscope.

Behavioral testing. The first batch of NMUR2 KO and WT littermate mice were tested in a battery of "primary screen" behavioral assays in the following order: 24-h home cage activity with body weight and food intake, open field activity, hot plate, light-dark box, tail suspension, prepulse inhibition, and contextual fear conditioning. The testing order was predetermined, with less stressful tests conducted before more stressful ones. There was at least 1 day of rest between tests. Additional batches of mice were used to replicate any near-significant findings and for more tests, including elevated plus maze, formalin test, feeding studies, and i.c.v. injections of NMU peptide. Each batch of mice consists of 15 to 18 WT and 15 to 18 KO mice to ensure sufficient statistical power against variation of behavioral data.

Open field activity was monitored in VersaMax chambers (Accuscan Instruments, Columbus, OH) measuring 40 by 40 cm and detected by infrared photobeam breaks. Mice were monitored in the chamber for 20 min. Measurements used to assess locomotor activity include horizontal activity, total distance traveled, vertical activity, rotation, stereotypy, and distance traveled in the center compared to total distance traveled (center/total distance ratio).

The light-dark box is divided into a brightly lit compartment (27 cm by 20 cm by 30 cm) and a dark compartment (18 cm by 20 cm by 30 cm), with an opening in between to allow the mouse access to both compartments. The mouse was placed in the light-dark box for 6 min, during which the timing of each transition from the dark to light or light to dark compartments, defined as all four limbs of the animal crossing the boundary, was recorded using The Observer Mobile with a Psion Workabout (Noldus Information Technology, The Netherlands).

The elevated plus maze (Med Associates, St. Albans, VT) is elevated 50 cm above the floor. A video camera mounted above the maze is used to record the animal's behavior. A mouse was placed in the central platform, facing an open arm, and allowed free exploration in the maze for 5 min. Using an automated video tracking software ANY-maze (Stoelting, Wood Dale, IL), the following criteria were measured: number of entries into open or closed arms, time spent in open or closed arms, entries into the distal portion of open arms, and head-dipping over sides of open arms, etc.

The tail suspension test uses an automated tail suspension apparatus (Med Associates). A mouse was taped by the tail to the hook of the apparatus for 6 min. The load cell amplifier detected the animal's movements (struggle to escape), and the immobility time (when the animal was not struggling) was measured as the animal's movement below a preset threshold.

The prepulse inhibition of the acoustic startle response was tested using the SR-Lab System (San Diego Instruments, San Diego, CA). A test session consists of six trial types under the background noise of 70 dB. One type uses a 40-ms, 120-dB noise as the acoustic startle stimulus. Four types contain the startle stimulus preceded by acoustic prepulses of different intensity: the 20-ms prepulse noise of 73, 76, 79, or 82 dB is presented 100 ms before the 120-dB startle stimulus. The last trial type uses the 70-dB background noise with no startle stimulus to measure baseline reaction. Six blocks of the six trial types were presented in pseudorandom order. Startle response was recorded for 65 ms starting with the onset of the startle stimulus. Measurements used to assess prepulse inhibition are the maximum startle amplitude and the percent inhibition of the startle response by each of the 4 prepulses.

Contextual fear conditioning was conducted over 2 days. In a training session, a mouse was placed in the conditioning chamber (Med Associates) and allowed to explore the environment. Two minutes later, a 75-dB white noise was turned on for 30 s. A 2-s, 0.6-mA scrambled electric shock was delivered through the metal grid floor at the end of the noise period. The noise and shock was repeated once more 2 min later. The mouse was tested 24 h later by placing it in the same chamber for 5 min without noise or shocks. Freezing behavior was automatically measured using the FreezeFrame system (Actimetrics, Wilmette, IL).

The hot plate test was carried out by placing a mouse on a 55°C hot plate (Accuscan Instruments) and measuring the latency of a hind limb response (shaking or licking). The maximum time allowed on the hot plate was 30 s to prevent tissue damage; if the animal did not respond within this time, the time of latency was recorded as 30 s.

For the formalin test, a mouse was placed into a clear Plexiglas container, with mirrors behind to ensure that the animal's paws can be seen from all angles, and allowed to acclimate for 30 min. Using a 50-μl Hamilton syringe equipped with 30-gauge needle, 20 μl of 5% formalin solution was injected under the skin of the dorsal side of the animal's right hindpaw. The mouse was immediately returned to its container, and timing was started. Four to eight mice in individual containers were tested at the same time. They were videotaped for 1 to 2 h, and the video was used for continuous scoring later. The time spent licking (or biting) the injected paw was scored in 5-min bins. The total licking time in the first 15 min is considered the phase I response and that from 15 to 60 min is the phase II response.

Statistics. Data were analyzed with Student's *t* test, one-way or two-way analysis of variance (ANOVA), or Mann-Whitney U test where appropriate, using the SPSS program (SPSS Inc, Chicago, IL). The significance level was set at a *P* value of <0.05. Data were presented as means ± standard errors of the means. *P* values reported were from one-way ANOVA or Student's *t* test unless otherwise indicated.

Intracerebroventricular injection. Freehand i.c.v. injection of mouse NMU-23 peptide (Phoenix Pharmaceuticals) was done while the mouse was anesthetized with an isoflurane vaporizer. A 27-gauge 1/2-inch-long needle fitted with a 0.8-cm plastic sheath (leaving a 0.4-cm needle tip exposed) was attached to a 10-μl Hamilton syringe. Slight pressure was applied to the ears in a downward direction to level and stabilize the head during injection. The injection was given into the lateral ventricle with the needle inserted perpendicularly to the head, 1.0-mm posterior of the bregma and 0.5-mm lateral to the midline. An initial hole was made 1 to 7 days before the beginning of the study and validated with angiotensin II-induced drinking behavior. All further injections were made through the same hole. After a slow continuous injection, the needle remained in place for several seconds, allowing the solution to disperse and preventing backflow up the needle track. NMU-23 was freshly dissolved in artificial cerebrospinal fluid (aCSF) (Harvard Apparatus, Holliston, MA) and injected in a volume of 2 to 4 μl.

Blood chemistry. Blood was collected via retro-orbital eye bleeding, and centrifuged in Microtainer tubes (Becton-Dickinson, Franklin Lakes, NJ) for plasma separation. Plasma was assayed for cholesterol, T4, triglyceride, and glucose using a Prochem V biochemistry analyzer (Drew Scientific, Oxford, CT). Leptin, insulin, and glucagon were measured by Linco Diagnostics (St. Charles, MO) using a Lincoplex luminex assay.

Histology. A standard Nissl staining protocol was used to evaluate neuronal density and general anatomical features. Brain or spinal cord sections were dehydrated in a standard series of alcohols (50, 70, 95, and 100%; 2 min each). Sections were then rehydrated in a series of alcohol solutions of decreasing concentrations (100, 95, 70, and 50%; 2 min each) and in distilled water for 5 min. This was followed by incubation of sections in a filtered solution containing 0.5% cresyl violet in distilled water for 5 min. Finally, sections were dehydrated in a series of alcohols, defatted in xylene, and coverslipped.

Whole-cell patch clamp recordings in spinal cord slices. Mice (4 to 9 weeks old) were anesthetized with isoflurane. Transverse slices of the lumbar spinal cord (300 μm) were prepared as described previously (38, 47). Slices were incubated in a solution containing 95 mM NaCl, 1.8 mM KCl, 1.2 mM KH_2PO_4, 0.5 mM $CaCl_2$, 7 mM $MgSO_4$, 26 mM $NaHCO_3$, 15 mM glucose, and 50 mM sucrose and oxygenated with 95% O_2–5% CO_2, pH 7.4 (osmolarity, 310 to 320 mosM). After a 1-h recovery, a single slice was transferred to a recording chamber on the stage of a BX51W1 microscope equipped with infrared differential interference contrast optics for patch clamp recordings with an Axon 200B amplifier (Axon Instruments, CA) and continuously superfused with oxygenated recording solution at 3 ml/min. The recording solution was identical to the incubation solution except for 127 mM NaCl, 2.4 mM $CaCl_2$, 1.3 mM $MgSO_4$, and 0 mM sucrose. The experiments were conducted at room temperature (21 to 25°C).

Spinal lamina II could be identified under the microscope as a translucent band capping the dorsal part of the gray matter. Because there is no clear demarcation between lamina IIo and III, we arbitrarily divided the lamina II into three equal zones from dorsal to ventral boundaries: outer, middle, and inner zones. All recordings in this study were restricted to neurons located in the outer zone. The resting membrane potential was measured immediately after establishing the whole-cell configuration. Only neurons that had an apparent resting membrane potential of more negative than −50 mV were investigated further. Hyperpolarizing (−20 pA) and depolarizing (20 to 160 pA in 20-pA steps) current injections of 0.8-s duration were applied to determine the firing pattern from the resting membrane potential. Recording electrodes (2 to 5 MΩ) contained a pipette solution composed of the following (in mM): 120 K-glucuronate, 5 NaCl, 1 $MgCl_2$, 0.5 EGTA, 2 Mg ATP, 0.1 Na_3GTP, 10 HEPES (pH 7.2, 280 to 300 mosM). Cs-$MeSO_3$ replaced K-glucuronate when inhibitory postsynaptic currents (IPSCs) were recorded. Spontaneous excitatory postsynaptic currents (sEPSCs) were recorded in the presence of bicuculline (10 μM) and strychnine (1 μM) to block GABA-A and glycine receptors at a holding potential of −70 mV, and spontaneous IPSCs (sIPSCs) were recorded in the presence of AP5 (50 μM) to block NMDA receptor at the holding potential of +10 mV. Access resistance was 15 to 40 MΩ and was monitored throughout the experiment. No correction for liquid potential was made. Recorded currents were filtered at 1 kHz and digitized at 10 kHz. Results were expressed as means ± standard errors of the means. Statistical comparisons were performed using the Student's *t* test.

RESULTS

Generation of NMUR2 KO mice. A mutant ES cell library constructed by infection with a retroviral vector (11, 12, 29) was screened for viral insertions in the *Nmur2* gene, and a mutant clone (Fig. 1A) was isolated and used to produce mice. The coding sequence of the *Nmur2* gene is located in 4 exons spanning the 16-kb genomic region (41). The virus was inserted in the third intron, as confirmed by sequencing and Southern blot analysis (data not shown). The retroviral vector contains a splice acceptor, termination codons in all reading frames, a selection marker, and a transcription terminator (11), and its insertion is expected to interrupt the transcript before exon 4, which contains sequences encoding TM7 of the 7-transmembrane domain and the C-terminal domain, resulting in a truncated, nonfunctional receptor. RT-PCR using primers spanning the insertion amplified a correct PCR product from WT but not homozygous mutant (KO) animal (Fig. 1B), confirming the interruption of *Nmur2* transcript in NMUR2 KO mice. To further confirm the functional null of NMUR2 protein, ^{125}I-NMU-23 peptide was used for a receptor binding study on spinal cord sections (Fig. 1C). ^{125}I-NMU-23 binding was strongly detected in outer layers (lamina I/IIo) of spinal dorsal horns in WT mice, as reported previously (51), but was absent in NMUR2 KO, demonstrating the functional inactivation of the receptor caused by the retroviral insertion. The specificity of this ^{125}I-NMU-23 binding is illustrated by the loss of signal in WT mice in the presence of excess unlabeled NMU-8 peptide.

NMUR2 KO mice display no significant changes in general behavior screening. To evaluate activity and anxiety, mice were tested for open field activity (Fig. 2A). The NMUR2 KO mice showed levels of activity similar to those of the WT mice throughout the 20-min testing period. There was no significant difference between NMUR2 KO and WT mice in the total distance traveled [$F_{(1,30)} = 0.79$, $P = 0.38$, repeated measures ANOVA], as well as in total vertical activities, stereotypy counts, and number of clockwise or counterclockwise rotations (data not shown). In addition, the ratio of distances traveled in the central versus the whole area, as a measure of the level of anxiety displayed by animals in the novel open arena, does not

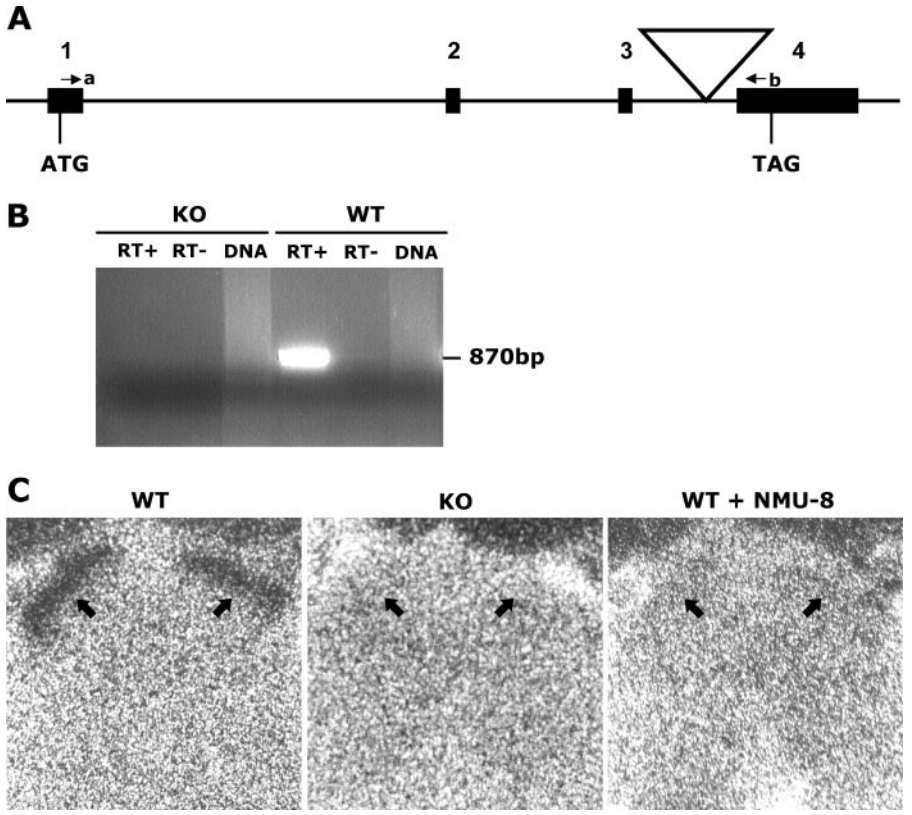

FIG. 1. Generation of NMUR2 KO mice. (A) Schematic diagram of the retroviral insertion in the *Nmur2* gene. Numbers 1 to 4 indicate coding exons, with the start codon (ATG) in exon 1 and the stop codon (TAG) in exon 4. The large triangle indicates the viral insertion. Primers a and b are indicated by small arrows. (B) RT-PCR using primers a and b, in which an 870-bp band is expected to be amplified from uninterrupted WT allele. RT+, reverse transcription reaction with the presence of reverse transcriptase. RT−, control reverse transcription reaction without reverse transcriptase. DNA, genomic DNA control in which no PCR band should be amplified because of large intronic regions between the two primers. (C) Receptor binding of ^{125}I-NMU-23 peptide to spinal cord transverse sections from WT and NMUR2 KO mice. Strong binding of ^{125}I-NMU-23 to the outer layers (indicated by arrows) of the spinal dorsal horn is detected in WT but not KO sections. Binding specificity is demonstrated by coincubating ^{125}I-NMU-23 with 1,000-fold excessive unlabeled NMU-8 peptide which results in a complete loss of signal in WT sections. Nonspecific signals in the bones surrounding the spinal cord (as seen partially at the top edges of the micrographs in all three sections) serve as anatomical reference points.

differ significantly between genotypes either [$F_{(1,30)} = 0.055$, $P = 0.82$, repeated measures ANOVA].

To further examine any changes in anxiety levels, the mice were subjected to the light-dark box and elevated plus maze tests. In the light-dark box test, less number of transitions between the light and dark compartments and more time spent in the dark compartment are two indicators for increased anxiety in animals. As shown in Fig. 2B, neither the number of transitions nor the total time spent in the dark was significantly different between NMUR2 KO and WT mice [$F_{(1,63)} = 0.14$, $P = 0.71$ and $F_{(1,63)} = 1.34$, $P = 0.25$, respectively]. In the elevated plus maze test, more-anxious animals would have a lower percentage of open arm entries and spend less time in the open arms, whereas the total number of entries into both open and closed arms reflects the animal's general locomotor activity. As shown in Fig. 2C, no significant differences were detected between NMUR2 KO and WT mice in the total number of arm entries, percentage of open arm entries, or total time spent in the open arms [$F_{(1,29)} = 0.49$, $P = 0.49$; $F_{(1,29)} = 0.15$, $P = 0.70$; $F_{(1,29)} = 0.011$, $P = 0.92$, respectively].

No significant differences were seen between NMUR2 KO and WT mice in the tail suspension test, a model of depression that measures a form of behavioral despair, prepulse inhibition that evaluates the sensorimotor gating function that is often disrupted in psychosis, and contextual fear conditioning, a measure of emotion-based associative learning and memory (data not shown).

NMUR2 KO mice have normal energy balance but do not respond to NMU's anorectic effect. Body weight and food consumption were measured daily for 3 days and were calculated as 3-day averages (Fig. 3A). There were no significant differences in body weight ($P = 0.23$, $n = 17$ KO, 17 WT) or basal food intake ($P = 0.26$, $n = 17$ KO, 16 WT) between WT and NMUR2 KO mice. Body weight was also measured in several additional batches of mice with ages ranging from 14 to 21 weeks old, and there were no differences between genotypes either (data not shown).

To assess endocrine status of the NMUR2 KO mice, blood chemistry was assayed for several metabolic hormones and fuels. No significant changes were noted for cholesterol, T4, leptin, insulin, glucagon, glucose, or triglycerides (Table 1) ($P > 0.05$ for all parameters). In addition, kidney and liver

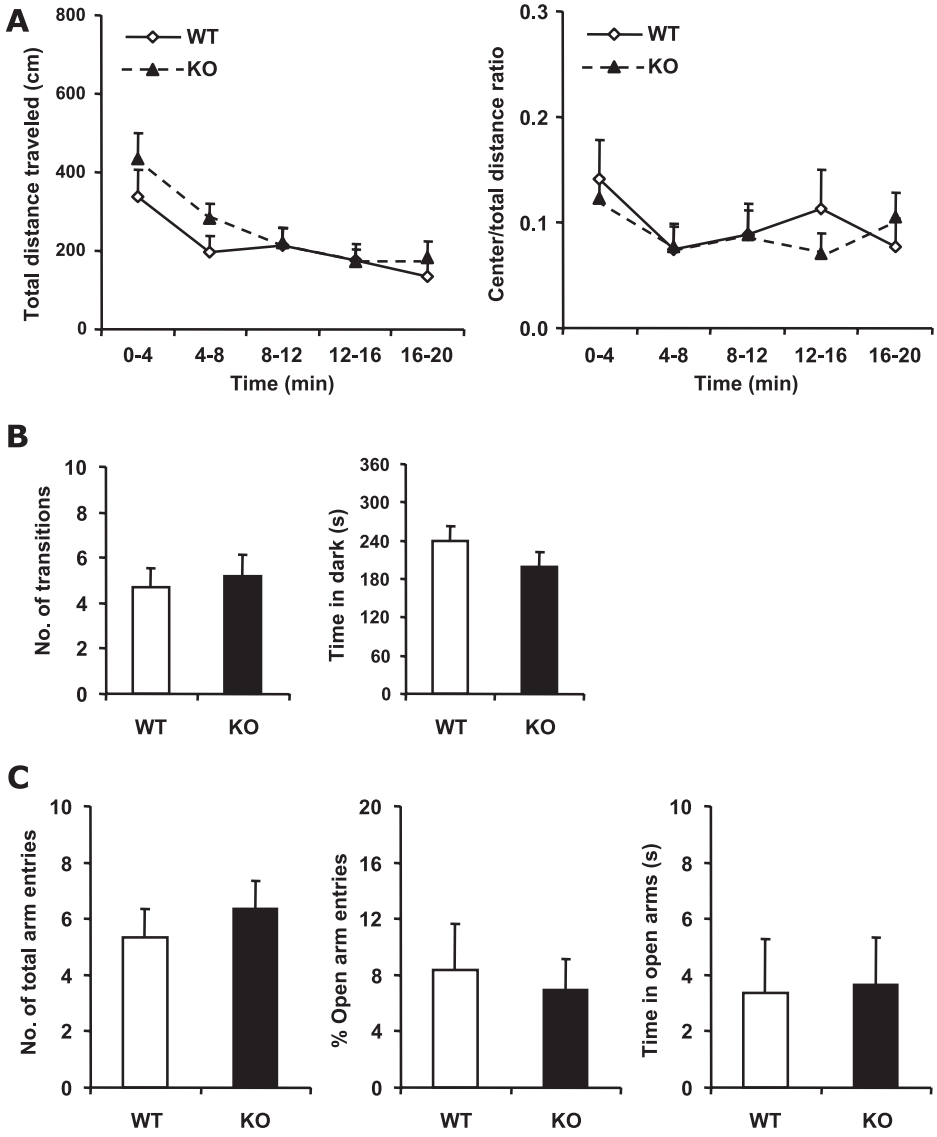

FIG. 2. Comparison of locomotor activity and anxiety between WT and NMUR2 KO mice. (A) Open field activity test. Activity levels are binned every 4 min. Left panel, total distance (in cm) traveled in the open field. Right panel, ratio of distance traveled in the center area versus the total distance traveled. (B) Light-dark box test. Left panel, total number of transitions between the light and dark compartments. Right panel, the time spent in the dark side during the 6-min testing period. (C) Elevated plus maze test. Left panel, total number of entries into both open and closed arms. Middle panel, percentage of entries into the open arms compared with total number of arm entries. Right panel, the time spent in the open arms during the 5-min testing period.

enzymes and electrolytes were normal in KO mice (data not shown).

To determine if inactivation of NMUR2 would make mice more sensitive to a metabolic challenge, their response to a 24-h fast was assessed (Fig. 3B). Both WT and KO mice lost an equivalent amount of weight during fasting, and both genotypes regained most of their original weight by 24 h postfast. However, the KO mice did regain less body weight than WT at the 24-h postfast time point ($P = 0.017$, $n = 18$ KO, 16 WT). This deficit was accompanied by a modest yet significant decrease in food intake relative to WT at both the 4-h and 24-h postfast time points ($P = 0.049$ and 0.001, respectively, $n = 18$ KO, 16 WT). This result is inconsistent with the postulated anorectic function of central NMU/NMUR2.

Mice were challenged with i.c.v. injections of NMU-23 to determine whether the previously reported central anorectic effects of this peptide are mediated primarily through the NMUR2 receptor. As shown in Fig. 3C, in WT animals, 5 nmol NMU-23 caused a significant reduction in overnight food intake compared to vehicle-treated WT mice ($P = 0.015$, $n = 8$ aCSF, 9 NMU-23) and a trend toward a reduction in body weight gain ($P = 0.099$, $n = 8$ aCSF, 9 NMU-23). In contrast, NMU-23 had no apparent effect in KO mice compared to vehicle-treated KO mice, on either body weight or food intake ($P = 0.81$ and 0.094, respectively, $n = 8$ aCSF, 9 NMU-23).

NMUR2 KO mice show decreased pain sensation and are refractory to NMU-induced nociceptive responses. (i) Decreased pain sensation in NMUR2 KO mice. In the hot plate

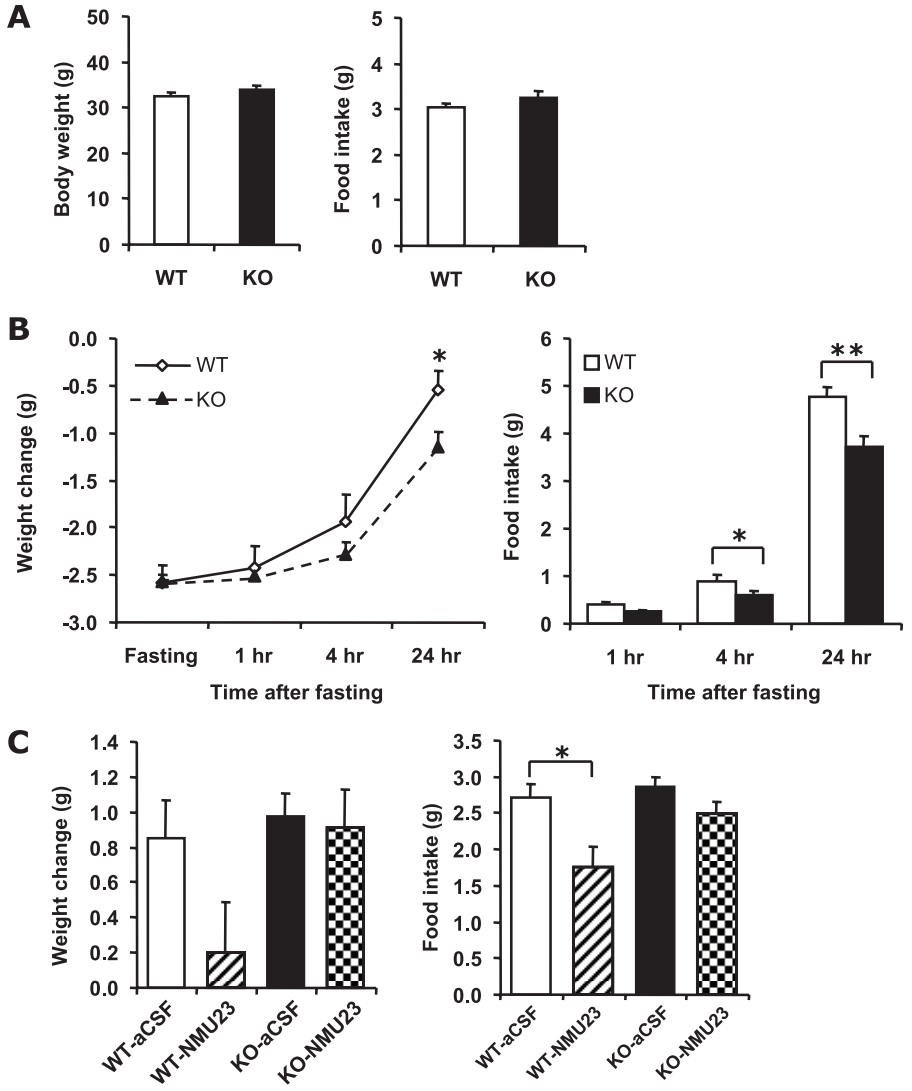

FIG. 3. Comparison of body weights and feeding behavior between WT and NMUR2 KO mice. (A) Body weights (left panel) and 24-h food intake (right panel) of 14- to 17-week-old mice. Each mouse was singly housed for a week before the measuring of body weight and food intake. (B) Fasting and refeeding test. Individually caged mice were fasted for 24 h starting at 1 p.m., with ad lib access to drinking water. Following fasting, mice were weighed and refed. Body weight changes (left panel) relative to prefasting levels and food intake (right panel) were monitored at 1, 4, and 24 h after the start of refeeding. (C) Body weight (left panel) and food intake (right panel) changes 15 h after i.c.v. injection of NMU-23 peptide. To stimulate appetite, mice were fasted for 5 h prior to injection, and NMU-23 (5 nmol in 4 μl aCSF) or vehicle (4 μl aCSF) was administered via i.c.v. injection at 6 p.m. (just before lights out). Food was given back right after injection. At 9 a.m. the following day, food intake and changes in body weight were measured. *, $P < 0.05$; **, $P < 0.01$.

TABLE 1. Blood chemistry of NMUR2 KO and WT mice

Parameter (unit)	Result (mean ± SEM) (*n*) for:	
	WT	NMUR2 KO
Cholesterol (mg/dl)	151 ± 12 (8)	169 ± 13 (7)
Glucagon (ng/ml)	0.11 ± 0.01 (17)	0.13 ± 0.01 (17)
Glucose (mg/dl)	183 ± 8 (8)	219 ± 15 (8)
Insulin (ng/ml)	2.3 ± 0.3 (17)	3.2 ± 0.5 (17)
Leptin (ng/ml)	3.3 ± 0.4 (17)	4.4 ± 0.5 (17)
T4 (μg/dl)	2.5 ± 0.5 (8)	3.3 ± 0.4 (8)
Triglycerides (mg/dl)	81 ± 9 (8)	92 ± 11 (8)

test, NMUR2 KO mice displayed a mild but consistent increase of the latency of the hindlimb shaking or licking response. To reduce variation and confirm this difference, each animal was tested on the hot plate three times over different days, and the latencies from the three trials were averaged. As shown in Fig. 4A, the latency was significantly longer in NMUR2 KO mice than in WT mice [$F_{(1,66)} = 8.79$, $P = 0.0044$].

The formalin model tests persistent pain produced by peripheral tissue injury and inflammation. The animal displays a biphasic response to the injection of formalin, a fast-onset sharp pain in phase I, and a slower-onset persistent pain in phase II that is related to inflammation and central sensitization. As shown in Fig. 4B, NMUR2 KO mice showed no dif-

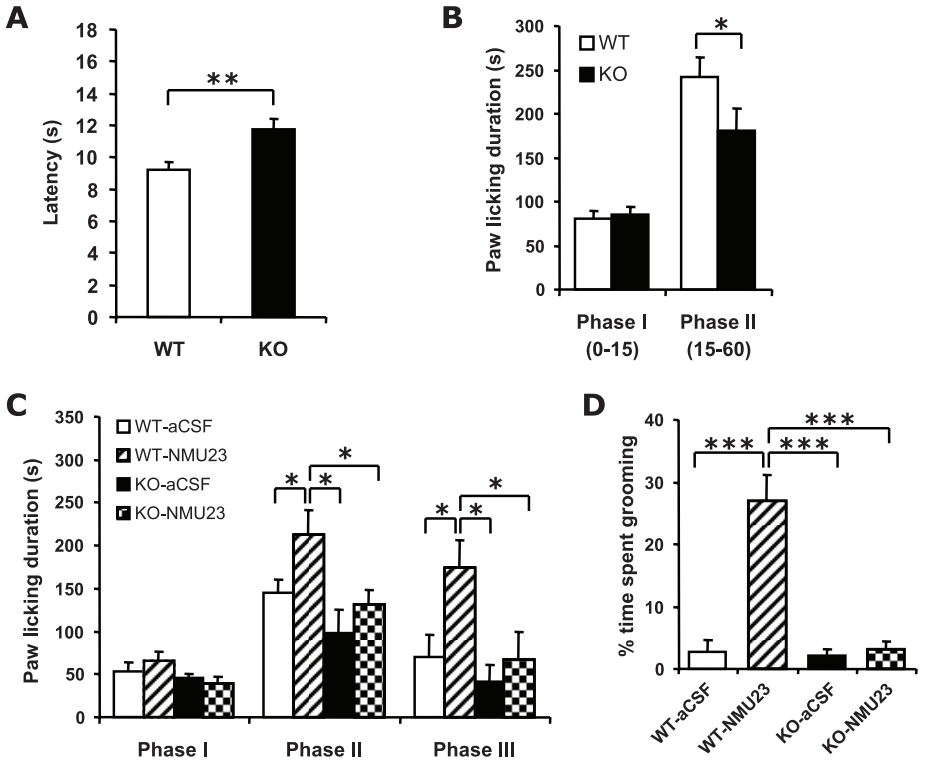

FIG. 4. Comparison of nociceptive responses between WT and NMUR2 KO mice. (A) Latencies of hind limb shaking or licking response in hot plate test. (B) Total time spent licking the injected paw in phase I (0 to 15 min after formalin injection) or phase II (15 to 60 min) of the formalin test. (C) Differential effects of NMU-23 in WT and NMUR2 KO mice in the formalin test. Shortly after i.c.v. injection of 3.5 nmol NMU-23 (in 3.5 μl aCSF) or vehicle (3.5 μl aCSF), the mice were placed in the testing container for acclimation for 30 min and then were injected with formalin solution at the right hind paw. The total time spent licking the injected paw in phase I, II, or III (60 to 105 min after formalin injection) is shown. (D) Excessive grooming or BSL behavior after i.c.v. injection of 3.5 nmol NMU-23. This behavior was scored from the videotapes during phase III of the formalin test described for panel C, i.e., 90 to 135 min after the i.c.v. injection, for the percentage of time spent in face-washing, licking or biting all over the body and tail (but excluding the specific licking or biting of the right hind paw injected with formalin solution). *, $P < 0.05$; **, $P < 0.01$; ***, $P < 0.001$.

ference in phase I response but a significant reduction in phase II response compared with WT mice ($P = 0.47$ and 0.040, respectively, Mann-Whitney U test, $n = 28$ KO, 28 WT).

(ii) Effects of centrally injected neuromedin U on pain sensation. To further determine if NMU-induced hyperalgesia is mediated by NMUR2, we examined the effects of centrally injected NMU-23 in the formalin test. In this case, we observed a prolonged hyperalgesic response in NMU-23-injected WT mice beyond the usual 60-min observation period. As a result, we extended the scoring period to include a phase III (60 to 105 min) (48), which is a continuation of phase II, to evaluate the long-lasting effect of NMU-23 on WT as well as NMUR2 KO mice. As shown in Fig. 4C, i.c.v. injection of 3.5 nmol NMU-23 in WT mice did not alter the phase I response but significantly increased the phase II and phase III responses compared to aCSF injection ($P = 0.39$, 0.050 and 0.024, respectively, $n = 8$ aCSF, 7 NMU-23). On the contrary, i.c.v. injection of 3.5 nmol NMU-23 in NMUR2 KO mice did not significantly change the pain responses in any of the three phases compared to aCSF injection ($P = 0.54$, 0.29, and 0.50, respectively, $n = 8$ aCSF, 9 NMU-23). Overall for phases II and III, there was a significant genotype effect and a significant treatment effect but not a significant genotype x treatment interaction [$F_{(1,28)} = 9.37$, $P = 0.0048$; $F_{(1,28)} = 7.33$, $P = 0.011$; $F_{(1,28)} = 1.67$, $P = 0.21$, respectively, two-way repeated measures ANOVA].

Similar to what has been reported previously for both rats (10, 15, 27, 45, 50, 51) and mice (4), we observed that i.c.v. injection of NMU-23 in WT mice induced an intense grooming-related behavior. This behavior was characterized by a series of excessive face washing, biting, and licking all over the body, including, in particular, the lower back, genital area, and tail, which may reflect an increased sensory input in the animals. Notably, this behavior was completely absent from the NMUR2 KO mice injected with NMU-23. Quantification of this excessive biting/scratching/licking (BSL) behavior (Fig. 4D) confirmed that WT mice injected with NMU-23 had significantly increased BSL behavior compared to aCSF-injected WT mice ($P < 0.001$, $n = 8$ aCSF, 7 NMU-23). On the other hand, there was no significant difference in the NMUR2 KO mice with or without NMU-23 injection ($P = 0.50$, $n = 8$ aCSF, 8 NMU-23). There were significant genotype effect, treatment effect, and genotype x treatment interactions [$F_{(1,27)} = 30.99$, $P < 0.001$; $F_{(1,27)} = 33.01$, $P < 0.001$; $F_{(1,27)} = 27.65$, $P < 0.001$, respectively, two-way ANOVA].

Effects of neuromedin U on synaptic transmission of spinal lamina IIo neurons. (i) Spinal cord morphology in wild-type and NMUR2 KO mice. Because nociceptive and other

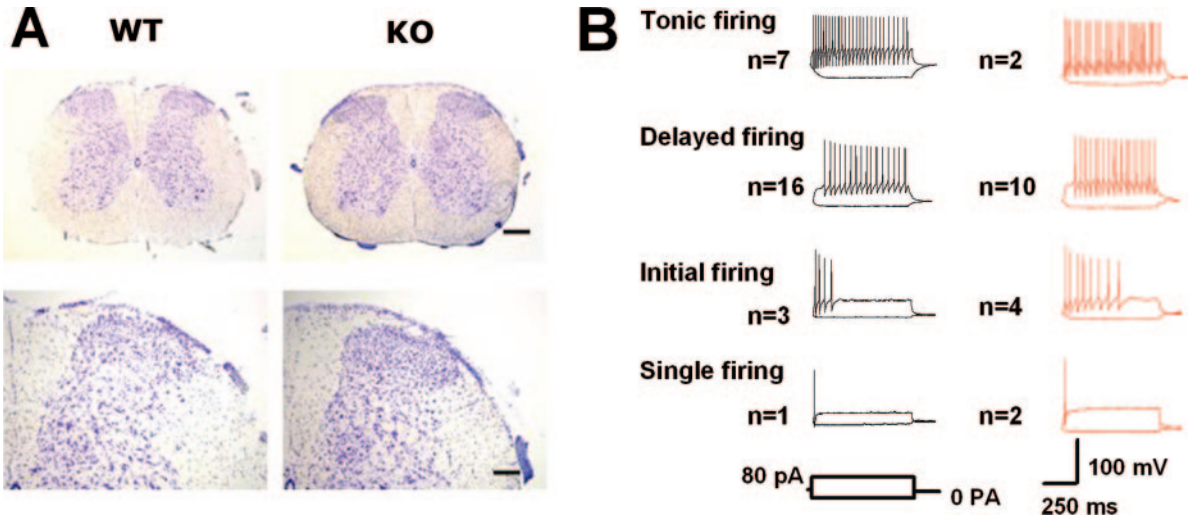

FIG. 5. Spinal cord morphology and firing patterns of spinal lamina IIo neurons. (A) Cresyl violet staining of lumbar spinal cord transverse sections. Upper panels, lower magnification; scale bar, 200 μm. Lower panels, higher magnification; scale bar, 80 μm. (B) Firing patterns of lamina IIo neurons from WT (traces in black) and NMUR2 KO (traces in red) mice. Twenty-nine WT neurons and 19 KO neurons are similarly categorized into 4 distinct types. No significant differences were revealed between WT and KO neurons in a number of membrane properties, including resting membrane potential (-61.0 ± 1.0 mV, $n = 29$, versus -63.4 ± 1.9 mV, $n = 19$), membrane resistance (482.4 ± 33.5 MΩ, $n = 29$, versus 516.5 ± 48.1 MΩ, $n = 19$), membrane capacitance (34.2 ± 1.5 pF, $n = 29$, versus 33.8 ± 2.4 pF, $n = 19$), and action potential threshold (-34.5 ± 1.7 mV, $n = 11$, versus -32 ± 1.9 mV, $n = 10$).

sensory responses to NMU are likely mediated in part by spinal cord neurons in the dorsal horn, we assessed the potential role of NMUR2 in spinal cord physiology. We first examined the morphology of the spinal cord by cresyl violet staining of serial transverse sections. There were no obvious differences in the number and distribution of neurons between WT and KO mice in the lumbar dorsal horn (Fig. 5A) as well as at the cervical, thoracic, and sacral levels (data not shown).

(ii) Firing patterns of spinal lamina IIo neurons. We performed whole-cell patch-clamp recordings in visually identified WT ($n = 29$) and NMUR2 KO ($n = 19$) neurons in lamina IIo in the spinal dorsal horn to study the resting membrane potential and firing pattern of these neurons (Fig. 5B). According to the categories of firing patterns in dorsal horn neurons defined by Ruscheweyh and Sandkuhler (38), 7 neurons displayed tonic firing, 16 neurons displayed delayed firing, 3 neurons displayed initial bursting, and 1 neuron displayed single spiking among the 29 WT neurons. Two of the recorded neurons could not be classified into any of these categories. Similarly, 2 neurons displayed tonic firing, 10 neurons displayed delayed firing, 4 neurons displayed initial bursting, and 2 neurons displayed single spiking among the 19 KO neurons. One of the recorded neurons could not be classified into any of these categories. No significant differences were revealed between WT and KO mice in a number of membrane properties ($P > 0.05$ in all measurements).

(iii) Effect of NMU-8 on sEPSCs in lamina IIo neurons. First we compared sEPSCs of lamina IIo neurons in WT and NMUR2 KO mice and found no difference in either frequency or amplitude ($P > 0.05$ in both cases, $n = 20$ WT, 14 KO) (Fig. 6A). To test whether NMU can regulate excitatory synaptic transmission, we examined the effect of NMU-8 on sEPSCs in lamina IIo neurons (Fig. 6B). An obvious rundown of sEPSC frequency was observed after the rupture of cells and during the whole-cell recording in lamina IIo neurons in WT slices. A similar rundown phenomenon of either glutamatergic or GABAergic neurotransmission has been reported in cultured hippocampal or cortical neurons (2, 26). However, after the bath application of NMU-8 (10 μM), the decrease of sEPSC frequency of the control was significantly reversed. Compared with the control value, the sEPSC frequencies of WT neurons ($n = 20$) in the presence of NMU-8 were significantly increased as follows: second minute, $128.7\% \pm 5.1\%$ ($P < 0.01$); third minute, $141.6\% \pm 6.3\%$ ($P < 0.01$); fourth minute, $130.6\% \pm 6.5\%$ ($P < 0.05$); fifth minute, $162.9\% \pm 11.0\%$ ($P < 0.05$); sixth minute, $149.4\% \pm 7.2\%$ ($P < 0.05$). No effect on sEPSC amplitude in the WT neurons ($P > 0.05$) was observed after the application of NMU-8. For NMUR2 KO neurons ($n = 14$), a similar rundown of sEPSC frequency during recording was observed. However, NMU-8 (10 μM) had no effect on either frequency or amplitude of sEPSCs ($P > 0.05$ for both).

(iv) Effect of NMU-8 on sIPSCs in lamina IIo neurons. When sIPSCs were compared in WT and NMUR2 KO mice, no difference was found in frequency or amplitude (Fig. 6C). We then examined the effect of NMU-8 on sIPSCs in lamina IIo neurons (Fig. 6D). The percent changes of sIPSC frequency in the presence of NMU-8 (10 μM) in the first, second, third, fourth, and fifth minutes were $106.8\% \pm 10.6\%$, $88.0\% \pm 5.0\%$, $102.3\% \pm 5.8\%$, $90.1\% \pm 17.2\%$, and $114.0\% \pm 21.4\%$ in WT neurons ($n = 5$). There were no significant differences in these time points in the absence and presence of NMU-8 ($P > 0.05$). Moreover, NMU-8 had no effect on sIPSC amplitude in the WT neurons ($P > 0.05$). In NMUR2 KO neurons, NMU-8 had no effect on either frequency ($P > 0.05$) or amplitude ($P > 0.05$) of sIPSCs.

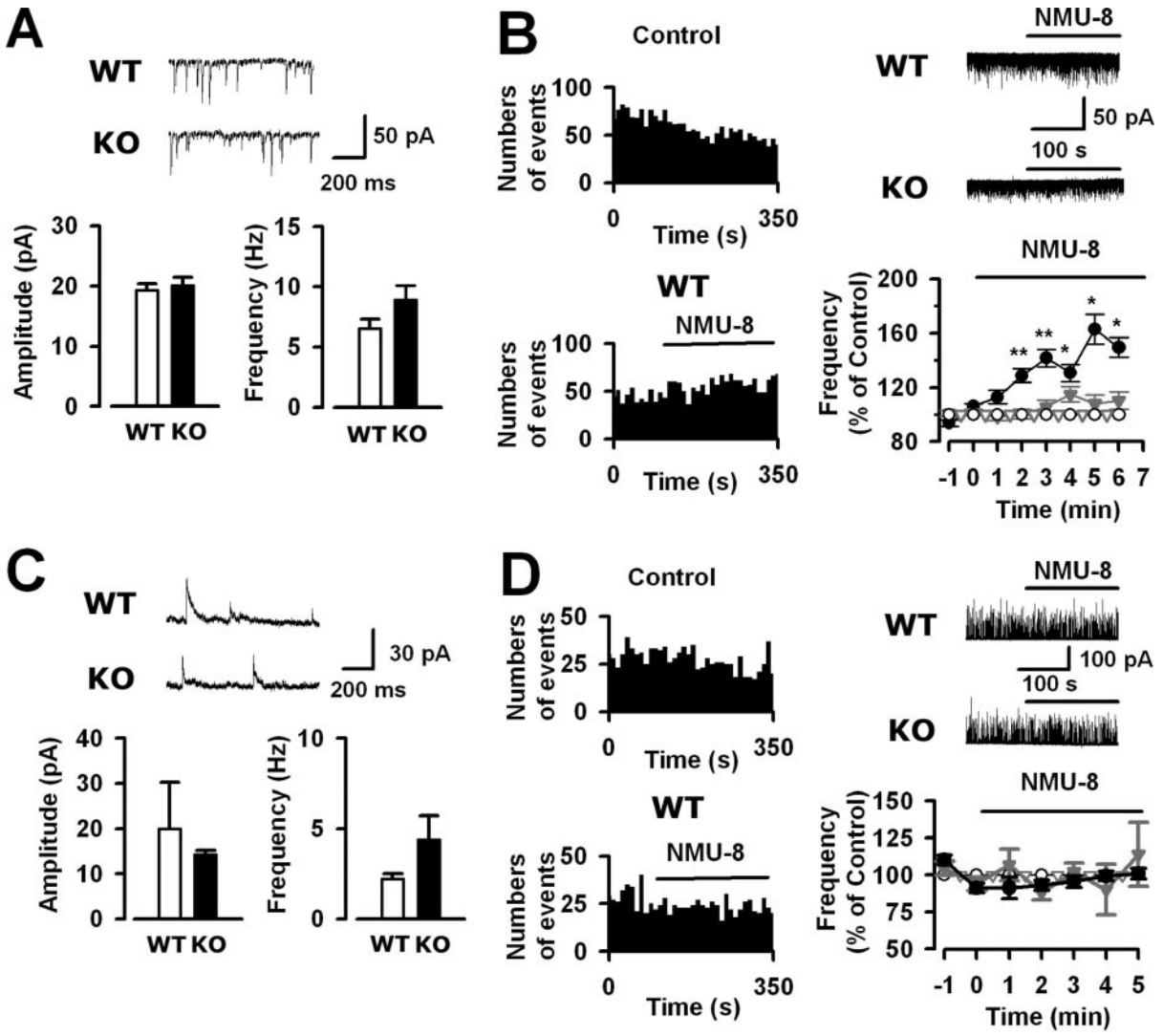

FIG. 6. Effects of NMU-8 on sEPSCs and sIPSCs of spinal lamina IIo neurons in WT and NMUR2 KO mice. (A) Spontaneous EPSCs of lamina IIo neurons: examples (upper traces) and average frequency and amplitude (lower panels). (B) Effect of NMU-8 (10 μM) on sEPSC frequency of lamina IIo neurons. Left panels, time course of WT neurons with control or NMU-8. Upper right panel, traces of WT and KO neurons with NMU-8. Lower right panel, percent change of sEPSC frequency after the application of NMU-8 in WT (black solid circles, $n = 20$) and KO (gray solid triangles, $n = 14$) relative to the normalized values in the absence of NMU-8 in WT (black open circles, $n = 9$) and KO (gray open triangles, $n = 5$). *, $P < 0.05$; **, $P < 0.01$ between WT NMU-8 and control curve. (C) Spontaneous IPSCs of lamina IIo neurons: examples (upper traces) and average frequency and amplitude (lower panels). (D) Effect of NMU-8 (10 μM) on sIPSC frequency of lamina IIo neurons. Left panels, time course of WT neurons with control or NMU-8. Upper right panel, traces of WT and KO neurons with NMU-8. Lower right panel, percent change of sIPSC frequency after the application of NMU-8 in WT (black solid circles, $n = 5$) and KO (gray solid triangles, $n = 4$) relative to the normalized values in the absence of NMU-8 in WT (black open circles, $n = 5$) and KO (gray open triangles, $n = 4$).

DISCUSSION

The present study shows that NMUR2 KO mice are phenotypically indistinguishable from WT mice in many behaviors, such as locomotor activity, mood and anxiety, sensorimotor gating, learning and memory, food intake, energy balance, and metabolism, but demonstrate specific alteration in pain sensitivity. This is in sharp contrast with the plethora of phenotypes exhibited by the NMU KO mice—most notably obesity, hyperphagia, hypometabolism, hypoactivity, reduced pain sensation, reduced stress response, and reduced inflammation (16, 32, 33). On the other hand, our study also shows that most effects of centrally administered NMU, such as increased nociceptive responses, enhanced excitatory synaptic transmission in spinal dorsal horn neurons, and decreased food intake, are mediated by the NMUR2 receptor. These results necessitate reevaluation of the roles of neuromedin U and its receptors in different physiological processes.

One consistent finding is that inactivation of both NMU and NMUR2 leads to reduced nociceptive responses. NMU KO mice (33) and NMUR2 KO mice (this study) both exhibit reduced pain sensitivity in the hot plate test and the chronic phase of the formalin test. Central administration of NMU-23 (via i.c.v. or i.t.) in rats or mice increases pain sensitivity, including thermal hyperalgesia in the tail immersion, hot plate,

and rat plantar tests, mechanical allodynia in the von Frey test, and increased phase II response in the formalin test (4, 33, 51). Here we also show that the increased pain responses in the formalin test induced by i.c.v. injection of NMU-23 are abolished in the NMUR2 KO mice. This finding together with the general reduction of pain sensitivity in the NMUR2 KO mice suggests that centrally released NMU peptide tonically increases pain sensation via the activation of NMUR2 receptor.

One of the major sites of NMU's effect on nociception is likely to lie within the spinal cord. NMU was first purified from a porcine spinal cord, and it has been found to be abundantly present in the spinal cord across many mammalian species (6, 19, 30, 42). *Nmu* is also expressed in sensory neurons in the DRG (31). Interestingly, radiolabeled NMU-23 shows highly specific binding sites in lamina I/IIo of the spinal dorsal horn, with little binding observed in other regions of the spinal cord or the DRG (51). Correspondingly, the *Nmur2* transcript is also highly localized to lamina IIo (and a few neurons in lamina I), whereas *Nmur1* is not detected in the spinal cord but in about 25% of small/medium-diameter neurons in the DRG (51). Lamina I/IIo is part of a major ascending nociceptive pathway from the spinal cord to the brainstem and then to higher brain regions, such as the hypothalamus and amygdala, and this pathway is believed to be more involved in the modulation of intensity and affective dimensions of pain than with the discriminative nature of the stimulus (5, 22). Several other neuropeptides, such as substance P and calcitonin-gene-related peptide, are also present in the lamina I area (46). It is intriguing that the NMUR2 KO mice exhibit selective reduction of pain responses in the late, but not early, phase of the formalin test under both basal and NMU-induced conditions, which is reminiscent of phenotypes observed in the TACR1 KO or TACR1-antagonist-treated mice (49), suggesting that NMU/NMUR2 may take part in central sensitization, similar to substance P. Moreover, in a mouse hindquarter preparation, systemic perfusion of NMU-23 potentiates both the background spiking rates and noxious pinch-evoked response of nociceptive or wide dynamic range but not nonnociceptive, dorsal horn neurons (4). In adult rat spinal cord slices, bath-applied NMU-23 increases the frequency, but not amplitude, of miniature EPSCs in lamina II and deep layer neurons without affecting miniature IPSCs (31). Similarly, here we have found that in adult mouse spinal cord slices, perfusion of NMU-8 increases the frequency, but not amplitude, of spontaneous EPSCs in lamina IIo neurons without affecting spontaneous IPSCs. Furthermore, we demonstrate that NMU-induced increase of sEPSC frequency of lamina IIo neurons is abolished in NMUR2 KO mice, further strengthening the notion that NMUR2 is a key mediator of NMU's effect in nociceptive sensory transmission.

To summarize, we have provided the following three lines of evidence that NMUR2 is the central mediator of NMU's pronociceptive effects: decreased intrinsic pain responses, absence of increased pain responses induced by centrally administered NMU, and abolished increase of sEPSC frequency induced by NMU in spinal cord slices. However, this conclusion does not exclude the possibility that NMU can also exert its nociceptive effects peripherally through NMUR1. In fact, it has been shown that NMU is involved in mast cell-mediated inflammation (32). NMU is present in the skin at high levels, and *Nmur1* is highly expressed in immune cells, including primary mast cells. Intraplantar injection of NMU into the paw induces early inflammatory responses such as mast cell degranulation, vasodilation, and plasma extravasation. Mast cell degranulation, edema, and neutrophil infiltration, induced by complete Freund's adjuvant injected into the paw, do not occur in NMU KO mice. Therefore, it is likely that NMU has a dual role in modulating the animal's response to noxious stimuli through its two receptors—enhancing both peripheral tissue injury-induced inflammation through NMUR1 and nociceptive sensory transmission in the spinal cord through NMUR2.

Central administration of NMU (via i.c.v. or i.t.) in rats or mice also induces a dramatic grooming or BSL behavior (4, 10, 15, 27, 45, 50, 51). This behavioral response is blocked by morphine and might be correlated with the bursting firing patterns of spinal neurons induced by NMU (4, 51), suggesting that it may be related to enhanced nociceptive sensory transmission. Here we show that the BSL behavior is completely abolished in the NMUR2 KO mice, supporting the role of NMUR2 in mediating this NMU-induced sensitization of sensory inputs. Intrathecal administration of many other pronociceptive agents, such as substance P (43), NMDA (40), nociceptin (39), and spermine (44), also produces similar characteristic BSL behavioral responses that are sensitive to analgesics. On the other hand, this behavior is also considered by others to be a stress-related response (15, 45, 50), which resembles the excessive grooming induced by i.c.v. injection of CRH or adrenocorticotrophin (7). This NMU-induced behavior is suppressed by a CRH antagonist or anti-CRH immunoglobulin G in rats (15). Direct injection of NMU into the hypothalamic PVN also increases grooming and locomotor behavior in rats (45, 50). We favor the interpretation that the BSL behavior primarily results from the activation of nociceptive pathways by NMU and in turn leads to other stress-related changes, such as increased plasma levels of stress hormones and increased c-Fos expression in brain areas associated with stress (10, 23, 35, 36, 50). This is based on the fact that the time course of onset of the BSL behavior in our NMU i.c.v. experiment was relatively slow, not starting until ~30 min after injection, compared with the earlier onset at 5 to 10 min post-i.t. injection of NMU in other studies (4, 51). This indicates that NMU's site of action may be in the spinal cord, since it may have taken some time for NMU to diffuse down to the spinal cord from the lateral ventricle where it was injected in our studies. Furthermore, it is generally believed that increased stress will lead to stress-induced analgesia (1); however, in our studies, hyperalgesia in the formalin test is observed along with the excessive BSL behavior after NMU administration, arguing against a primary stress response.

Our data neither support nor contradict the possibility that NMU and NMUR2 may also have a direct role in mediating stress responses. In rats, administration of NMU straight into hypothalamic PVN increases plasma levels of corticosterone, and NMU stimulates the release of CRH from hypothalamic explants in vitro (45, 50). In the NMU KO mice, several stress responses are attenuated, such as the blood pressure increase after the elevation of environmental temperature and the blood corticosterone level increase after immobilization stress (33). In our studies, NMUR2 KO mice do not behave differently from WT mice in several anxiety, depression, and fear-

related tests, i.e., open field activity, light-dark box, elevated plus maze, tail suspension, and contextual fear conditioning, suggesting that NMUR2 may not play a major role in anxiety and stress responses. In comparison, CRHR1 KO mice do display reduced anxiety behavior (reviewed in reference 25). It is apparent that more studies are needed to clarify the role of NMU and its receptors in the regulation of anxiety and stress.

Perhaps the most surprising finding from our studies is that, unlike the NMU KO mice, the NMUR2 KO mice do not develop obesity (up to ~5 months of age). It is believed that NMU is an anorectic peptide and is involved in the central control of feeding through its action in the hypothalamus, even though it is widely distributed throughout the body, with especially high levels in the gastrointestinal tract. Intracerebroventricular administration of NMU acutely suppresses food intake and body weight gain and stimulates energy expenditure in fasted rats (21, 23, 27, 34) and mice (17). Intra-PVN administration of NMU in rats has similar effects (50). Furthermore, these effects are all abolished in CRH KO mice, indicating that CRH is a major mediator of NMU's effect in feeding behavior and catabolic function (17). On the other hand, central injection of anti-NMU immunoglobulin G increases food intake (24, 27). However, all of these effects of NMU are transient, and it is not clear whether centrally acting NMU can have a long-term effect on body weight and energy balance. In fact, it has been shown that twice daily intra-PVN injection of NMU for 7 days does not alter an animal's food intake or body weight even though it does induce the typical excessive grooming behavior acutely and elevation of plasma corticosterone levels evident 18 h after the final injection (45). Genetic models provide some compelling evidence for the role of NMU in long-term energy homeostasis. NMU KO mice are hyperphagic, hypoactive, hypometabolic, and obese (16). They have elevated plasma insulin, leptin, total cholesterol, triglyceride and free fatty acid levels, and decreased expression of uncoupling proteins UCP1 and UCP3. In contrast, transgenic overexpression of NMU throughout the body leads to lean mice that are hypophagic and have improved glucose tolerance (28). However, in our current study, NMUR2 KO mice maintain normal body weight, normal daily food intake and normal plasma levels of endocrine hormones and energy metabolites. After a fasting challenge, NMUR2 KO mice are unexpectedly slower in the resumption of food and recovery of body weight, which is opposite to what one would have predicted from the notion that NMU has an anorectic effect based on previous studies. Therefore our results raise the possibility that the peripheral actions of NMU, mediated through NMUR1, rather than NMU's central actions through NMUR2, might be the major contributor to the long-term effects of NMU on energy homeostasis. Alternatively, there might be an unidentified receptor(s) that recognizes NMU or some other peptide derived from the precursor gene and mediates its central effects on energy balance.

Despite of the absence of major metabolic phenotypes in the NMUR2 KO mice, we have shown that acute suppression of food intake by central administration of NMU is abolished in the NMUR2 KO mice. This is consistent with a role (disputed in the previous paragraph) for NMUR2 in mediating NMU's central effect on feeding behavior. Alternatively, the suppression of food intake may be a secondary consequence of the increased nociceptive and stress responses induced by NMU. In any case, it is conceivable that both peripheral NMUR1 and central NMUR2 receptors, and perhaps yet another unidentified receptor(s), may be required for NMU to exert its effects in energy homeostasis. It might be that the unidentified receptor(s) responds to physiological concentrations of NMU, whereas NMUR2 responds to pharmacological doses (administered via i.c.v.). It is also possible that while NMUR2 can mediate NMU's acute anorectic effect, the long-term effects of NMU in maintaining the animal's energy homeostasis involve other individual receptor or combination of all these receptors.

ACKNOWLEDGMENTS

We thank Terry Reisine, Clifford Saper, and Olivier Civelli for comments on the manuscript. We are grateful to Kellie McIlwain for work in setting up some of the behavioral tests.

This work was supported by private funding and in part by an SBIR phase I grant from NIMH (MH070241) to A.G.

All authors affiliated with Nura, Inc., or Omeros Corporation hereby declare a potential conflict of financial interest.

REFERENCES

1. **Amit, Z., and Z. H. Galina.** 1986. Stress-induced analgesia: adaptive pain suppression. Physiol. Rev. **66:**1091–1120.
2. **Arancio, O., E. R. Kandel, and R. D. Hawkins.** 1995. Activity-dependent long-term enhancement of transmitter release by presynaptic 3′,5′-cyclic GMP in cultured hippocampal neurons. Nature **376:**74–80.
3. **Brighton, P. J., P. G. Szekeres, and G. B. Willars.** 2004. Neuromedin U and its receptors: structure, function, and physiological roles. Pharmacol. Rev. **56:**231–248.
4. **Cao, C. Q., X. H. Yu, A. Dray, A. Filosa, and M. N. Perkins.** 2003. A pro-nociceptive role of neuromedin U in adult mice. Pain **104:**609–616.
5. **Craig, A. D.** 1996. An ascending general homeostatic afferent pathway originating in lamina I. Prog. Brain Res. **107:**225–242.
6. **Domin, J., M. A. Ghatei, P. Chohan, and S. R. Bloom.** 1987. Neuromedin U–a study of its distribution in the rat. Peptides **8:**779–784.
7. **Dunn, A. J., C. W. Berridge, Y. I. Lai, and T. L. Yachabach.** 1987. CRF-induced excessive grooming behavior in rats and mice. Peptides **8:**841–844.
8. **Fujii, R., M. Hosoya, S. Fukusumi, Y. Kawamata, Y. Habata, S. Hinuma, H. Onda, O. Nishimura, and M. Fujino.** 2000. Identification of neuromedin U as the cognate ligand of the orphan G protein-coupled receptor FM-3. J. Biol. Chem. **275:**21068–21074.
9. **Funes, S., J. A. Hedrick, S. Yang, L. Shan, M. Bayne, F. J. Monsma, Jr., and E. L. Gustafson.** 2002. Cloning and characterization of murine neuromedin U receptors. Peptides **23:**1607–1615.
10. **Gartlon, J., P. Szekeres, M. Pullen, H. M. Sarau, N. Aiyar, U. Shabon, D. Michalovich, K. Steplewski, C. Ellis, N. Elshourbagy, M. Duxon, T. E. Ashmeade, D. C. Harrison, P. Murdock, S. Wilson, A. Ennaceur, A. Atkins, C. Heidbreder, J. J. Hagan, A. J. Hunter, and D. N. Jones.** 2004. Localisation of NMU1R and NMU2R in human and rat central nervous system and effects of neuromedin-U following central administration in rats. Psychopharmacology (Berlin) **177:**1–14.
11. **Gatanaris, G. A.** 8 May 2001. Vectors and methods for the mutagenesis of mammalian genes. U.S. patent US6228639B1.
12. **Gottsch, M. L., H. Zeng, J. G. Hohmann, D. Weinshenker, D. K. Clifton, and R. A. Steiner.** 2005. Phenotypic analysis of mice deficient in the type 2 galanin receptor (GALR2). Mol. Cell. Biol. **25:**4804–4811.
13. **Graham, E. S., Y. Turnbull, P. Fotheringham, K. Nilaweera, J. G. Mercer, P. J. Morgan, and P. Barrett.** 2003. Neuromedin U and neuromedin U receptor-2 expression in the mouse and rat hypothalamus: effects of nutritional status. J. Neurochem. **87:**1165–1173.
14. **Guan, X. M., H. Yu, Q. Jiang, L. H. Van Der Ploeg, and Q. Liu.** 2001. Distribution of neuromedin U receptor subtype 2 mRNA in the rat brain. Brain Res. Gene Expr Patterns **1:**1–4.
15. **Hanada, R., M. Nakazato, N. Murakami, S. Sakihara, H. Yoshimatsu, K. Toshinai, T. Hanada, T. Suda, K. Kangawa, S. Matsukura, and T. Sakata.** 2001. A role for neuromedin U in stress response. Biochem. Biophys. Res. Commun **289:**225–228.
16. **Hanada, R., H. Teranishi, J. T. Pearson, M. Kurokawa, H. Hosoda, N. Fukushima, Y. Fukue, R. Serino, H. Fujihara, Y. Ueta, M. Ikawa, M. Okabe, N. Murakami, M. Shirai, H. Yoshimatsu, K. Kangawa, and M. Kojima.** 2004. Neuromedin U has a novel anorexigenic effect independent of the leptin signaling pathway. Nat. Med. **10:**1067–1073.
17. **Hanada, T., Y. Date, T. Shimbara, S. Sakihara, N. Murakami, Y. Hayashi, Y. Kanai, T. Suda, K. Kangawa, and M. Nakazato.** 2003. Central actions of

neuromedin U via corticotropin-releasing hormone. Biochem. Biophys. Res. Commun. **311:**954–958.
18. **Hedrick, J. A., K. Morse, L. Shan, X. Qiao, L. Pang, S. Wang, T. Laz, E. L. Gustafson, M. Bayne, and F. J. Monsma, Jr.** 2000. Identification of a human gastrointestinal tract and immune system receptor for the peptide neuromedin U. Mol. Pharmacol. **58:**870–875.
19. **Honzawa, M., T. Sudoh, N. Minamino, M. Tohyama, and H. Matsuo.** 1987. Topographic localization of neuromedin U-like structures in the rat brain: an immunohistochemical study. Neuroscience **23:**1103–1122.
20. **Hosoya, M., T. Moriya, Y. Kawamata, S. Ohkubo, R. Fujii, H. Matsui, Y. Shintani, S. Fukusumi, Y. Habata, S. Hinuma, H. Onda, O. Nishimura, and M. Fujino.** 2000. Identification and functional characterization of a novel subtype of neuromedin U receptor. J. Biol. Chem. **275:**29528–29532.
21. **Howard, A. D., R. Wang, S. S. Pong, T. N. Mellin, A. Strack, X. M. Guan, Z. Zeng, D. L. Williams, Jr., S. D. Feighner, C. N. Nunes, B. Murphy, J. N. Stair, H. Yu, Q. Jiang, M. K. Clements, C. P. Tan, K. K. McKee, D. L. Hreniuk, T. P. McDonald, K. R. Lynch, J. F. Evans, C. P. Austin, C. T. Caskey, L. H. Van der Ploeg, and Q. Liu.** 2000. Identification of receptors for neuromedin U and its role in feeding. Nature **406:**70–74.
22. **Hunt, S. P., and P. W. Mantyh.** 2001. The molecular dynamics of pain control. Nat. Rev. Neurosci. **2:**83–91.
23. **Ivanov, T. R., C. B. Lawrence, P. J. Stanley, and S. M. Luckman.** 2002. Evaluation of neuromedin U actions in energy homeostasis and pituitary function. Endocrinology **143:**3813–3821.
24. **Jethwa, P. H., C. J. Small, K. L. Smith, A. Seth, S. J. Darch, C. R. Abbott, K. G. Murphy, J. F. Todd, M. A. Ghatei, and S. R. Bloom.** 2005. Neuromedin U has a physiological role in the regulation of food intake and partially mediates the effects of leptin. Am. J. Physiol. Endocrinol. Metab. **289:**E301–E305.
25. **Keck, M. E., F. Ohl, F. Holsboer, and M. B. Muller.** 2005. Listening to mutant mice: a spotlight on the role of CRF/CRF receptor systems in affective disorders. Neurosci. Biobehav. Rev. **29:**867–889.
26. **Kittler, J. T., G. Chen, S. Honing, Y. Bogdanov, K. McAinsh, I. L. Arancibia-Carcamo, J. N. Jovanovic, M. N. Pangalos, V. Haucke, Z. Yan, and S. J. Moss.** 2005. Phospho-dependent binding of the clathrin AP2 adaptor complex to GABAA receptors regulates the efficacy of inhibitory synaptic transmission. Proc. Natl. Acad. Sci. USA **102:**14871–14876.
27. **Kojima, M., R. Haruno, M. Nakazato, Y. Date, N. Murakami, R. Hanada, H. Matsuo, and K. Kangawa.** 2000. Purification and identification of neuromedin U as an endogenous ligand for an orphan receptor GPR66 (FM3). Biochem. Biophys. Res. Commun. **276:**435–438.
28. **Kowalski, T. J., B. D. Spar, L. Markowitz, M. Maguire, A. Golovko, S. Yang, C. Farley, J. A. Cook, G. Tetzloff, L. Hoos, R. A. Del Vecchio, T. M. Kazdoba, M. F. McCool, J. J. Hwa, L. A. Hyde, H. Davis, G. Vassileva, J. A. Hedrick, and E. L. Gustafson.** 2005. Transgenic overexpression of neuromedin U promotes leanness and hypophagia in mice. J. Endocrinol. **185:**151–164.
29. **Krasnow, S. M., J. G. Hohmann, A. Gragerov, D. K. Clifton, and R. A. Steiner.** 2004. Analysis of the contribution of galanin receptors 1 and 2 to the central actions of galanin-like peptide. Neuroendocrinology **79:**268–277.
30. **Minamino, N., K. Kangawa, and H. Matsuo.** 1985. Neuromedin U-8 and U-25: novel uterus stimulating and hypertensive peptides identified in porcine spinal cord. Biochem. Biophys. Res. Commun **130:**1078–1085.
31. **Moriyama, M., H. Furue, T. Katafuchi, H. Teranishi, T. Sato, T. Kano, M. Kojima, and M. Yoshimura.** 2004. Presynaptic modulation by neuromedin U of sensory synaptic transmission in rat spinal dorsal horn neurones. J. Physiol. **559:**707–713.
32. **Moriyama, M., T. Sato, H. Inoue, S. Fukuyama, H. Teranishi, K. Kangawa, T. Kano, A. Yoshimura, and M. Kojima.** 2005. The neuropeptide neuromedin U promotes inflammation by direct activation of mast cells. J. Exp. Med. **202:**217–224.
33. **Nakahara, K., M. Kojima, R. Hanada, Y. Egi, T. Ida, M. Miyazato, K. Kangawa, and N. Murakami.** 2004. Neuromedin U is involved in nociceptive reflexes and adaptation to environmental stimuli in mice. Biochem. Biophys. Res. Commun. **323:**615–620.
34. **Nakazato, M., R. Hanada, N. Murakami, Y. Date, M. S. Mondal, M. Kojima, H. Yoshimatsu, K. Kangawa, and S. Matsukura.** 2000. Central effects of neuromedin U in the regulation of energy homeostasis. Biochem. Biophys. Res. Commun. **277:**191–194.
35. **Niimi, M., K. Murao, and T. Taminato.** 2001. Central administration of neuromedin U activates neurons in ventrobasal hypothalamus and brainstem. Endocrine **16:**201–206.
36. **Ozaki, Y., T. Onaka, M. Nakazato, J. Saito, K. Kanemoto, T. Matsumoto, and Y. Ueta.** 2002. Centrally administered neuromedin U activates neurosecretion and induction of c-fos messenger ribonucleic acid in the paraventricular and supraoptic nuclei of rat. Endocrinology **143:**4320–4329.
37. **Raddatz, R., A. E. Wilson, R. Artymyshyn, J. A. Bonini, B. Borowsky, L. W. Boteju, S. Zhou, E. V. Kouranova, R. Nagorny, M. S. Guevarra, M. Dai, G. S. Lerman, P. J. Vaysse, T. A. Branchek, C. Gerald, C. Forray, and N. Adham.** 2000. Identification and characterization of two neuromedin U receptors differentially expressed in peripheral tissues and the central nervous system. J. Biol. Chem. **275:**32452–32459.
38. **Ruscheweyh, R., and J. Sandkuhler.** 2002. Lamina-specific membrane and discharge properties of rat spinal dorsal horn neurones in vitro. J. Physiol. **541:**231–244.
39. **Sakurada, T., S. Katsuyama, S. Sakurada, M. Inoue, K. Tan-No, K. Kisara, C. Sakurada, H. Ueda, and J. Sasaki.** 1999. Nociceptin-induced scratching, biting and licking in mice: involvement of spinal NK1 receptors. Br. J. Pharmacol. **127:**1712–1718.
40. **Sakurada, T., Y. Manome, K. Tan-No, S. Sakurada, and K. Kisara.** 1990. The effects of substance P analogues on the scratching, biting and licking response induced by intrathecal injection of N-methyl-D-aspartate in mice. Br. J. Pharmacol. **101:**307–310.
41. **Shan, L., X. Qiao, J. H. Crona, J. Behan, S. Wang, T. Laz, M. Bayne, E. L. Gustafson, F. J. Monsma, Jr., and J. A. Hedrick.** 2000. Identification of a novel neuromedin U receptor subtype expressed in the central nervous system. J. Biol. Chem. **275:**39482–39486.
42. **Szekeres, P. G., A. I. Muir, L. D. Spinage, J. E. Miller, S. I. Butler, A. Smith, G. I. Rennie, P. R. Murdock, L. R. Fitzgerald, H. Wu, L. J. McMillan, S. Guerrera, L. Vawter, N. A. Elshourbagy, J. L. Mooney, D. J. Bergsma, S. Wilson, and J. K. Chambers.** 2000. Neuromedin U is a potent agonist at the orphan G protein-coupled receptor FM3. J. Biol. Chem. **275:**20247–20250.
43. **Takahasi, K., T. Sakurada, S. Sakurada, H. Kuwahara, A. Yonezawa, R. Ando, and K. Kisara.** 1987. Behavioural characterization of substance P-induced nociceptive response in mice. Neuropharmacology **26:**1289–1293.
44. **Tan-No, K., A. Taira, K. Wako, F. Niijima, O. Nakagawasai, T. Tadano, C. Sakurada, T. Sakurada, and K. Kisara.** 2000. Intrathecally administered spermine produces the scratching, biting and licking behaviour in mice. Pain **86:**55–61.
45. **Thompson, E. L., K. G. Murphy, J. F. Todd, N. M. Martin, C. J. Small, M. A. Ghatei, and S. R. Bloom.** 2004. Chronic administration of NMU into the paraventricular nucleus stimulates the HPA axis but does not influence food intake or body weight. Biochem. Biophys. Res. Commun. **323:**65–71.
46. **Todd, A. J., and R. C. Spike.** 1993. The localization of classical transmitters and neuropeptides within neurons in laminae I-III of the mammalian spinal dorsal horn. Prog. Neurobiol. **41:**609–645.
47. **Wei, F., K. I. Vadakkan, H. Toyoda, L. J. Wu, M. G. Zhao, H. Xu, F. W. Shum, Y. H. Jia, and M. Zhuo.** 2006. Calcium calmodulin-stimulated adenylyl cyclases contribute to activation of extracellular signal-regulated kinase in spinal dorsal horn neurons in adult rats and mice. J. Neurosci. **26:**851–861.
48. **Wei, F., G. D. Wang, G. A. Kerchner, S. J. Kim, H. M. Xu, Z. F. Chen, and M. Zhuo.** 2001. Genetic enhancement of inflammatory pain by forebrain NR2B overexpression. Nat. Neurosci. **4:**164–169.
49. **Woolf, C. J., R. J. Mannion, and S. Neumann.** 1998. Null mutations lacking substance: elucidating pain mechanisms by genetic pharmacology. Neuron **20:**1063–1066.
50. **Wren, A. M., C. J. Small, C. R. Abbott, P. H. Jethwa, A. R. Kennedy, K. G. Murphy, S. A. Stanley, A. N. Zollner, M. A. Ghatei, and S. R. Bloom.** 2002. Hypothalamic actions of neuromedin U. Endocrinology **143:**4227–4234.
51. **Yu, X. H., C. Q. Cao, F. Mennicken, C. Puma, A. Dray, D. O'Donnell, S. Ahmad, and M. Perkins.** 2003. Pro-nociceptive effects of neuromedin U in rat. Neuroscience **120:**467–474.